

# Local densities, distribution functions, and wave function correlations for spatially resolved shot noise at nanocontacts

Thomas Gramesbacher and Markus Büttiker

Département de Physique Théorique, Université de Genève, CH-1211, Genève 4, Switzerland  
(February 1, 2008)

We consider a current-carrying, phase-coherent multi-probe conductor to which a small tunneling contact is attached. We treat the conductor and the tunneling contact as a phase-coherent entity and use a Green's function formulation of the scattering approach. We show that the average current and the current fluctuations at the tunneling contact are determined by an *effective local non-equilibrium distribution function*. This function characterizes the distribution of charge-carriers (or quasi-particles) inside the conductor. It is an exact quantum-mechanical expression and contains the phase-coherence of the particles via local partial densities of states, called *injectivities*. The distribution function is analyzed for different systems in the zero-temperature limit as well as at finite temperature. Furthermore, we investigate in detail the correlations of the currents measured at two different contacts of a four-probe sample, where two of the probes are only weakly coupled contacts. In particular, we show that the correlations of the currents are at zero-temperature given by spatially *non-diagonal* injectivities and emissivities. These non-diagonal densities are sensitive to correlations of wave functions and the phase of the wave functions. We consider ballistic conductors and metallic diffusive conductors. We also analyze the Aharonov-Bohm oscillations in the shot noise correlations of a conductor which in the absence of the nano-contacts exhibits no flux-sensitivity in the conductance.

PACS numbers: 61.16.Ch, 73.20.At, 72.70.+m

## I. INTRODUCTION

To measure the properties of a system it is necessary to couple a measurement apparatus to the system. To minimize the effect that the presence of the measurement apparatus has on the properties of the system, it is desirable to have the coupling as weak as possible. We are interested in the properties of a current carrying, phase-coherent multi-probe conductor. Weak coupling or non-invasive contacts on mesoscopic conductors were already used by Engquist and Anderson [1] to re-derive Landauer's resistance formula [2] for a small conductor with a scatterer. Here we are interested in weak coupling contacts which are sensitive to the phase of current amplitudes [3–5] and not only as in the work of Engquist and Anderson and related work [6] to absolute values of currents. Nowadays, the scanning tunneling microscope (STM) [7] is a very powerful experimental realization of a weakly coupled contact. Due to the fact that the tunneling current to the tip originates only from an atomically small area on the surface below the tip, it has become the standard tool to measure the local electronic structure on the surface of conductors. In experiment, it is possible to map the topography of a surface with atomic resolution [8,9]. Standing electron wave patterns confined to quantum corrals [10], which were constructed by manipulation of single atoms, or on carbon nanotubes serving as a one-dimensional electron box [11] are clearly visible using a low-temperature STM.

In the theoretical description, initially Tersoff and Hamann [12] used the Bardeen approach to tunneling [13] to relate the tunneling conductance to the local density

of states (LDOS)  $\nu(x)$  on the surface of the conductor. Recently, Bracher *et al.* [14] arrived at the same result using a propagator theory where the tip was described as a localized source or sink of electrons. These approaches have been used to interpret many of the features encountered in STM images. In theory and experiment, the STM has most often been used in a two-terminal configuration, the two terminals being the tip on one side and the conductor on the other. The current at the tip is then determined by the two-terminal conductance between tip and surface, and is given by the Bardeen formula [13],  $G_{ts} = (e^2/h)4\pi^2\nu_{tip}|t|^2\nu(x)$ , with the LDOS  $\nu(x)$  of the sample,  $\nu_{tip}$  of the tunneling tip, and the coupling energy  $|t|$ . The zero-bias conductance thus measures directly the LDOS  $\nu(x)$  on the surface of the conductor below the tip.

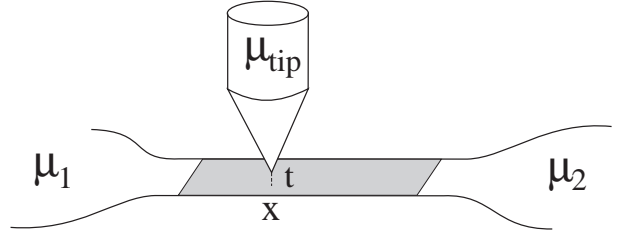


FIG. 1. Experimental setup to measure the effective local distribution function. The tip of an STM couples at a point  $x$  with a coupling strength  $t$  to the surface of a multi-terminal conductor. The contacts of the conductor are held at potentials  $\mu_\alpha$  and the tip at potential  $\mu_{tip}$ . This configuration can be used to measure the time dependent current or voltage at the tip.

In this article, we make theoretical predictions for measurements using one (or two) tunneling tips on mesoscopic phase-coherent multi-probe conductors and analyze the voltage and the current fluctuations measured at such a contact. The proposed experimental setup is shown in Figs. 1 and 2. The current at the tips is now determined by all conductances between the tip and the massive contacts of the sample. Applying a bias at the massive contacts of the multi-probe conductor one can drive already a current through it without the presence of the tunneling contacts. This puts the conductor into a non-equilibrium state. Here we are interested in the characterization of the transport state. The STM is used to measure the electronic structure on the surface of the current carrying sample. We will see later that the average current and the current fluctuation spectrum at a single tunneling tip are determined by an *effective local non-equilibrium distribution function* expressed as a function of local partial densities of states (LPDOS) and the Fermi distribution functions in the electron reservoirs. A measurement of such a distribution, averaged over a spatially wide area, has been performed by Pothier *et al.* [15] using a large superconducting tunneling contact on a metallic diffusive wire. We are interested in characterizing the transport state not only locally but also by its spatial and temporal correlations. The measurement of the correlations of the currents at *two* different tunneling tips is related to spatially non-diagonal densities of states and can give information about correlations of wave functions and the phase of the wave functions.

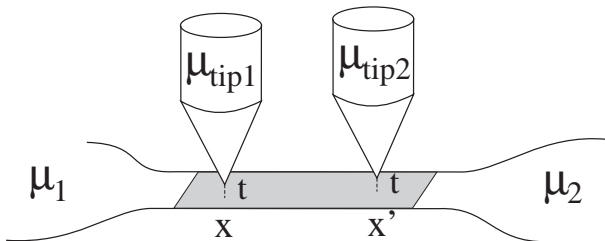


FIG. 2. Experimental setup to measure current correlations. Two STM tips are coupled with strength  $t$  at the positions  $x$  and  $x'$  to the surface of a small wire. The shaded region can be a metallic diffusive or a perfect ballistic wire.

Here, we use a fully phase-coherent theory of weak coupling contacts starting from the overall scattering matrix which includes the conductor and the tunneling contacts as one entity. A fully phase-coherent discussion of four-probe resistances measured with weakly coupled contacts has been presented in Ref. [4]. In this work and in recent work by the two of us [5] such an approach has been used to investigate the local voltage measurements and phase-coherent resistance measurements on mesoscopic wires. Of particular interest is the relationship of the transmission probabilities to densities of states which characterize the conductor. In the transport problem of interest here it is shown [5] that the densities of states which ap-

pear are partial densities of states, called *injectivity* for transmission from a contact of the conductor into the tip, and called *emissivity* for the transition from the tip into one of the contacts of the conductor. The transmission probabilities from the sample into the tip and from the tip into the sample can be viewed as a generalization of the well known Bardeen expression for the two-terminal weak coupling contact [5]. The generalized densities of states, the injectivity and emissivity play a fundamental role also in the dynamic conductance of mesoscopic systems [16,17] and in the non-linear conductance of mesoscopic systems [18,19].

In the following, we use the same approach but extend the discussion to treat temporal current and voltage fluctuations and investigate the correlations of currents measured at two tunneling contacts. As we will show later, these measurements can reveal more information about the electronic structure than can be found by pure conductance measurements. At elevated temperature and with an applied bias the fluctuations of the currents can be divided into two contributions: the thermal noise, which is proportional to the temperature and an excess noise, called shot-noise, which is only present when the system is biased [20,21]. The thermal noise is via a fluctuation-dissipation theorem related to a conductance and does therefore not contain more information about the conductor than can be drawn from measuring conductances. However, the shot-noise, which is at zero-temperature the only source of fluctuations, can give more information [20]. For instance, the shot-noise spectrum can be used to distinguish between different conductance mechanisms, such as ballistic or diffusive conductance [21]. The low-frequency shot-noise spectrum has been used to identify the fractional charge of the quasi-particles in the fractional quantum Hall regime [22,23], and, recently, van den Brom and van Ruitenbeek [24] used combined conductance and shot-noise measurements to determine the detailed mechanism of the electrical conductance through atom-size metallic gold-contacts. Birk *et al.* [25] measured the shot noise at an STM tip. Of particular interest are current-current cross-correlations [26,20,27] due to their sensitivity to the statistics of the carriers. Specific predictions have been made for current correlations of conductors in high quantizing magnetic fields [26,20,27], for ballistic conductors [28], for metallic diffusive conductors with massive contacts [29,30], for chaotic cavities [31], and for hybrid normal and superconducting systems [32]. Very recently, measurements of current cross-correlations (the electric analog of the Hanbury Brown Twiss experiment) have been reported by Henny *et al.* [33] for a Hall bar geometry which permits the separation of incident and reflected carrier streams as suggested in Ref. [26] and by Oliver *et al.* [34] for a conductor that exhibits probably elements both of ballistic electron motion and chaotic electron motion. More severe tests of our understanding of fluctuations arise from probing exchange effects in correlations due to the quantum mechanical indistinguishability of

identical particles. We will discuss exchange effects below in some detail. Earlier discussions of exchange effects in cross-correlations in mesoscopic conductors can be found in Refs. [35,20,27,29–32]. An experiment which investigates exchange effects in the noise at a single contact due to two incident carrier streams has been carried out by Liu et al. [36]. Therefore, we believe it to be justified to assume, that the shot-noise measurements at local tunneling contacts proposed in this work can in fact be done as well.

In order to be able to make statements about the local structure or wave function correlations on the sample surface, the contact between tip and sample should be local in the sense that tunneling occurs only over a region which is small compared to the variation of the LDOS on the surface of the conductor. In general, this length scale is given by the Fermi wavelength of the surface states. Modern STM measurements show clearly that atomic resolution on metallic surfaces can be achieved using sufficiently sharp tips. In addition, STM tips have the advantage that they can be moved around on a surface so that it is possible to draw entire *maps* of e. g. the LDOS and to study the spatial variation of the transport and noise properties. The theory we formulate below, however, is also valid for spatially fixed contacts provided the contact is sufficiently small and in the regime of tunneling. Especially, for the experiment with two tunneling contacts, Fig. 2, it might practically be much easier to use a setup with one spatially fixed tunneling contact and one (movable) STM tip.

We note that some of the results presented below have already been published in a shortened version in [37].

## II. HAMILTONIAN FORMULATION OF THE SCATTERING MATRIX AND THE L(P)DOS

We are concerned with open mesoscopic systems consisting of a finite part where electrons are scattered and to which  $N$  huge, macroscopic electron reservoirs are attached. The phase coherence length for the electrons is supposed to be much longer than the spatial dimensions of the scattering region. Then, inelastic scattering takes only place in the electron reservoirs. In each reservoir  $\alpha$  the electrons are in equilibrium and distributed according to a Fermi function characterized by the electro-chemical potential  $\mu_\alpha$  and the temperature  $T_\alpha$ . The finite scattering region is described by a Hamiltonian  $H_C$  and the connection to the electron reservoirs is modeled by semi-infinite ideal leads described by a Hamiltonian  $H_L$ . As a basis of the Hamiltonian  $H_C$  we choose  $M$  localized states  $|x\rangle$  (where  $M$  is a very big number),

$$H_C = \sum_{x,x'} |x\rangle H_{xx'} \langle x'|. \quad (1)$$

The Hilbert space of the semi-infinite leads is spanned by scattering states  $|\alpha m\rangle$  totally reflected at the bound-

ary to the scattering region. At an energy  $E$  we have to sum over the scattering states of all open channels in the leads,

$$H_L = \sum_{\alpha=1}^N \sum_{m=1}^{N_\alpha} |\alpha m\rangle E \langle \alpha m|. \quad (2)$$

The index  $\alpha$  gives the number of the reservoir and the index  $m$  is the channel number of the incoming electron. In reservoir  $\alpha$  there are  $N_\alpha$  open channels at the energy  $E$ . Finally, we have to describe the coupling between the scattering states in the ideal leads and the conductor by a coupling matrix

$$W = \sum_x \sum_{\alpha=1}^N \sum_{m=1}^{N_\alpha} |x\rangle W_{x,\alpha m} \langle \alpha m|. \quad (3)$$

The Hamiltonian of the entire system then reads

$$\mathcal{H} = H_L + H_C + W + W^\dagger. \quad (4)$$

The Green's function between two points  $x$  and  $x'$  inside the scattering region is then at the Fermi-energy  $E_F$  given by [38]

$$G(x, x') = \langle x | (E_F - H_C + i\pi W W^\dagger)^{-1} | x' \rangle. \quad (5)$$

The matrix elements of the scattering matrix  $s_{\alpha m, \beta n}$ , which describes the scattering of an incoming particle in channel  $n$  of contact  $\beta$  being scattered into channel  $m$  of contact  $\alpha$ , can be written as

$$s_{\alpha m, \beta n} = \delta_{\alpha\beta} \delta_{mn} - 2\pi i \sum_{x, x'} W_{x, \alpha m}^* G(x, x') W_{x', \beta n}. \quad (6)$$

The scattering matrix depends on the electrostatic potential  $U(x)$  in the scattering region which is included in the Hamiltonian  $H_C$ . This potential has in principle to be calculated self-consistently for the system in equilibrium [16]. A small variation  $\delta\mu_\alpha$  of the electro-chemical potential in a reservoir  $\alpha$  injects then at a position  $x$  inside the conductor an additional charge [39]  $q(x) = e\nu(x, \alpha)\delta\mu_\alpha$ . The proportionality factor  $\nu(x, \alpha)$  is a LPDOS and is called the injectivity of contact  $\alpha$  at the point  $x$ . It can be expressed with the help of the scattering matrix as [17]

$$\nu(x, \alpha) = \frac{-1}{2\pi i} \sum_{\beta} \text{Tr} \left( \mathbf{s}_{\beta\alpha}^\dagger \frac{\delta \mathbf{s}_{\beta\alpha}}{e\delta U(x)} \right) \quad (7)$$

Here,  $\mathbf{s}_{\alpha\beta}$  denotes the  $N_\alpha \times N_\beta$  sub-matrix of the scattering matrix which describes the scattering of electrons between all channels of contacts  $\alpha$  and  $\beta$ . With the Green's function defined above, we have for the injectivity the expression [5]

$$\nu(x, \alpha) = \langle x | G T_\alpha G^\dagger | x \rangle, \quad (8)$$

where we introduced the abbreviation

$$\Gamma_\alpha = \sum_{x,x'} |x\rangle\langle x'| \sum_{m=1}^{N_\alpha} W_{x,\alpha m} W_{x',\alpha m}^* \quad (9)$$

Using the Lippmann-Schwinger equation  $|\psi_{\alpha m}\rangle = (1 - GW)|\alpha m\rangle$  which relates the scattering state  $|\psi_{\alpha m}\rangle$  of the entire coupled system to the scattering states  $|\alpha m\rangle$  of the isolated leads [38], one can express the injectivity in terms of the scattering wave functions

$$\nu(x, \alpha) = \sum_{m=1}^{N_\alpha} \frac{1}{\hbar v_{\alpha m}} |\psi_{\alpha m}(x)|^2 \quad (10)$$

Here,  $v_{\alpha m} = \sqrt{2/m^*(E_F - E_{\alpha m}^0)}$  is the velocity of an incoming electron at the Fermi energy  $E_F$  in channel  $m$  of contact  $\alpha$ ,  $m^*$  is the effective electron mass and  $E_{\alpha m}^0$  is the threshold energy of channel  $m$  of contact  $\alpha$ .

Related to the injectivity is another LPDOS, the emissivity  $\nu(\beta, x)$  of a point  $x$  into contact  $\alpha$ , defined as

$$\nu(\beta, x) = \frac{-1}{2\pi i} \sum_\alpha \text{Tr} \left( \mathbf{s}_{\beta\alpha}^\dagger \frac{\delta \mathbf{s}_{\beta\alpha}}{e \delta U(x)} \right) \quad (11)$$

and in terms of Green's functions given by

$$\nu(\beta, x) = \langle x | G^\dagger \Gamma_\beta G | x \rangle. \quad (12)$$

If there is a magnetic field  $B$  present, the injectivity and emissivity obey the symmetry [17]

$$\nu_B(\alpha, x) = \nu_{-B}(x, \alpha). \quad (13)$$

That means, reversing the magnetic field turns the injectivity of a specific contact into its emissivity and vice versa. As a special case, Eq. (13) states that injectivity and emissivity are the same if there is no magnetic field present. Furthermore, the emissivity can according to Eq. (10) and (13) be expressed in terms of the scattering states of the Hamiltonian with the reversed magnetic field. The LDOS  $\nu(x)$  is the sum of the injectivities of all contacts or the emissivities of all contacts,

$$\nu(x) = \sum_\alpha \nu(x, \alpha) = \sum_\beta \nu(\beta, x). \quad (14)$$

The LDOS is therefore invariant under reversal of the magnetic field.

The form of Eqs. (8) and (12) suggests to define a non-diagonal two-point injectivity by

$$\nu(x', x, \alpha) = \langle x' | G \Gamma_\alpha G^\dagger | x \rangle \quad (15)$$

$$= \sum_{m=1}^{N_\alpha} \frac{1}{\hbar v_{\alpha m}} \psi_{\alpha m}(x') \psi_{\alpha m}(x)^* \quad (16)$$

and analogously a non-diagonal two-point emissivity by

$$\nu(\beta, x', x) = \langle x' | G^\dagger \Gamma_\beta G | x \rangle. \quad (17)$$

In fact, we will see that it is exactly these spatially non-diagonal LPDOS which determine the correlation of the currents at two tips.

### III. SCATTERING MATRIX FORMULATION OF CURRENT AND NOISE

Our goal is to investigate the local electronic structure of a mesoscopic phase-coherent multi-probe conductor using one or several locally weakly coupled probes such as e. g. STM tips. One can think of transport experiments which measure the average current determined by conductances or one can measure the fluctuations of the current away from its average. The scattering matrix approach has proven to be very useful in describing transport and noise measurements at multi-probe conductors [40]. It provides us with formulae which express the currents and the fluctuations of the currents at the contacts of a multi-probe conductor in terms of its scattering matrix and the Fermi functions  $f_\alpha(T, E)$  of the electron distribution in the reservoirs. The experimentally directly accessible parameters of the system are the temperature  $T$  and the electro-chemical potentials  $\mu_\alpha$  in the large electron reservoirs.

For a certain temperature  $T$  and given potentials the average current flowing from contact  $\alpha$  into the conductor is [20]

$$\langle I_\alpha \rangle = \frac{e}{h} \sum_\beta \int dE \text{Tr} [A_{\beta\beta}(\alpha)] f_\beta(E) \quad (18)$$

with the current matrix  $A_{\delta\gamma}(\alpha) = \mathbf{1}_\alpha \delta_{\alpha\delta} \delta_{\alpha\gamma} - \mathbf{s}_{\alpha\delta}^\dagger(E) \mathbf{s}_{\alpha\gamma}(E)$ . The energy dependent transmission probability between two different contacts  $\alpha$  and  $\beta$  is  $T_{\alpha\beta} = -\text{Tr}[A_{\beta\beta}(\alpha)]$ . In the limit of zero temperature and if we assume that the differences of the applied potentials are so small that the scattering matrix depends only very weakly on energy in the energy interval of interest, formula (18) reduces to

$$\langle I_\alpha \rangle = \frac{e}{h} \sum_\beta T_{\alpha\beta} (\mu_\alpha - \mu_\beta), \quad (19)$$

where the transmission probabilities  $T_{\alpha\beta}$  have to be evaluated at the Fermi energy.

The correlation spectrum  $\langle \Delta I_\alpha \Delta I_\beta \rangle$  of the currents at two contacts  $\alpha$  and  $\beta$  is the Fourier transform of the current-current correlator [21],

$$\langle \Delta I_\alpha \Delta I_\beta \rangle = \int dt e^{i\omega t} \langle \Delta I_\alpha(t) \Delta I_\beta(t + t_0) \rangle, \quad (20)$$

where  $\Delta I_\alpha(t) = I_\alpha(t) - \langle I_\alpha \rangle$ . In the low-frequency limit,  $\omega \rightarrow 0$ , one gets [20]

$$\langle \Delta I_\alpha \Delta I_\beta \rangle = \frac{2e^2}{h} \sum_{\delta\gamma} \int dE \text{Tr} [A_{\delta\gamma}(\alpha) A_{\gamma\delta}(\beta)] f_\delta(1 - f_\gamma). \quad (21)$$

For  $\alpha = \beta$  this expression gives the low-frequency fluctuation spectrum of the current at the contact  $\alpha$ . For  $\alpha \neq \beta$  it gives the correlation-spectrum of the currents in the two contacts  $\alpha$  and  $\beta$ . In general, the current fluctuation- or correlation-spectrum is a mixture of thermal noise and, if the system is biased, an excess noise called shot-noise. At zero temperature all fluctuations in the currents are due to the discreteness of the charge carriers. We are dealing with pure shot-noise. At a given instant in time a carrier either arrives at a reservoir, i. e. a current is measured, or it does not. Successive carriers that are totally uncorrelated give the full (Poissonian) shot-noise,  $S_{Pois} = 2e|I|$ . If successive carriers are correlated, as is the case for electrons due to Fermi statistics, the noise can be suppressed below this value.

Eq. (21) gives the fluctuation spectrum of the time-dependent currents in the contacts under the condition that the potentials at the reservoirs are held fixed and do not fluctuate. This corresponds to the case where currents are measured using a zero-impedance external circuit. Alternatively, we could measure the voltages at the reservoirs using ideal, infinite impedance voltmeters. The infinite impedance external circuit then forces the currents to be zero at all times,  $I(t) = 0$ . Fluctuations in the currents have therefore to be counterbalanced by fluctuations of the chemical potentials in the electron reservoirs. In linear response to the applied bias, current and potential are related by a conductance matrix  $G_{\alpha\beta}$ ,

$$I_\alpha(t) = \sum_\beta G_{\alpha\beta}(V_\beta + \Delta V_\beta(t)) + \Delta I_\alpha(t), \quad (22)$$

where the  $\Delta I_\alpha(t)$  are now considered as Langevin forces obeying the correlation spectra given in Eq. (21) and where we allowed the potential at the reservoirs to be time dependent.

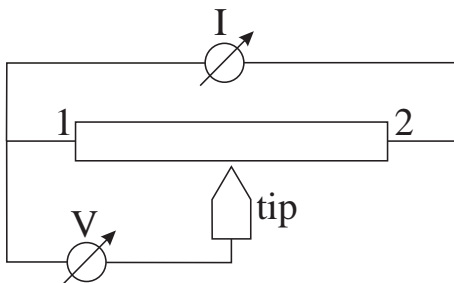


FIG. 3. Experimental setup to measure the voltage fluctuations at the tip. The voltage is measured using an infinite impedance voltmeter between contact 1 and the tip, and the current is measured using a zero-impedance ampere-meter between contacts 1 and 2.

Let us now consider the experimental setup of Fig. 3. We are interested in the fluctuations of the voltage at the tip  $\langle(\Delta V_{tip})^2\rangle$  measured relative to the voltage at contact 1. The current at the tip is always zero,  $I_{tip}(t) = 0$ , whereas at the contacts 1 and 2 the potentials are fixed,

$\Delta V_1(t) = \Delta V_2(t) = 0$ . We measure all voltages relative to the potential at contact 1 (freedom of the choice of gauge) so that  $V_1 = 0$ . Solving the system of equations (22) for  $\Delta V_{tip}(t)$  gives

$$\Delta V_{tip}(t) = -\frac{1}{G_{31} + G_{32}} \Delta I_{tip}(t) \quad (23)$$

and the fluctuation spectrum

$$\langle(\Delta V_{tip})^2\rangle = \left(\frac{1}{G_{31} + G_{32}}\right)^2 \langle(\Delta I_{tip})^2\rangle. \quad (24)$$

Eqs. (18), (21) and (24) are our starting points and we apply them to systems consisting of a conductor with two (or more) massive contacts and one or two weakly coupled contacts as depicted in Figs. 1 and 2. Our plan is to start with the scattering matrix of the entire system (sample and tip) and expand this scattering matrix in powers of the coupling strength  $|t|$  of the tip to the conductor. In this way we get equations which contain the scattering matrices of the separated systems, one describing scattering only in the sample and one describing the scattering in the tip.

Here, we use the Hamiltonian formulation to express the scattering matrix in terms of the Green's function of the mesoscopic sample, Eq. (6). Representing the scattering matrix in terms of Green's functions is a comfortable way to identify the (non-diagonal) density operators, Eqs. (15) and (17), in the expressions for the conductances and the current-correlation spectra.

#### IV. THE SINGLE TIP CONFIGURATION

We consider a system consisting of a mesoscopic conductor connected to  $N$  electron reservoirs and which has one additional weakly coupling contact, the tunneling tip (see e. g. Fig. 1 where  $N = 2$ ). The coupling strength between the tip and the conductor is  $|t|$  and the coupling is local at a point  $x$  on the surface of the conductor.

##### A. Average current at the tip

The transmission probability at an energy  $E$  for an electron incoming from a massive contact  $\alpha$  of the sample being transmitted into the tip has been found to be proportional to the injectivity of the contact at the coupling point  $x$  of the tip [5],

$$T_{tip,\alpha} = 4\pi^2 \nu_{tip} |t|^2 \nu(x, \alpha). \quad (25)$$

The transmission probability for an electron incoming from the tip being scattered into a massive contact  $\alpha$  is proportional to its emissivity [5],

$$T_{\alpha,tip} = 4\pi^2 \nu(\alpha, x) |t|^2 \nu_{tip}. \quad (26)$$

Due to the symmetry of injectivity and emissivity, Eq. (13), these transmission probabilities manifestly obey the Onsager-Casimir symmetry,  $T_{tip,\alpha}(B) = T_{\alpha,tip}(-B)$ , where  $B$  is the magnetic field. Using these energy resolved transmission probabilities in Eq. (18) we can express the average current flowing into the tip as

$$\langle I_{tip} \rangle = \frac{e}{h} \int dE T_{ts}(x) \{ f_{tip}(E) - f_{eff}(x) \} \quad (27)$$

with the two-probe tip-to-sample transmission  $T_{ts}(x) = 4\pi^2 \nu_{tip} |t|^2 \nu(x)$  and the *effective local distribution function*

$$f_{eff}(x) = \sum_{\alpha=1}^N \frac{\nu(x, \alpha)}{\nu(x)} f_{\alpha}(E). \quad (28)$$

This expression gives the local non-equilibrium distribution of charge carriers at the point  $x$  inside the conductor. Its energy dependence comes from the Fermi functions and from a possible energy dependence of the L(P)DOS.

Eq. (27) has the form of the current in a two probe system, one probe being the tip, where the electron distribution is described by the Fermi function  $f_{tip}(E)$  and the other probe where the electron distribution is given by the effective distribution function  $f_{eff}(x)$ . This effective distribution function does not account for any energy relaxation of the charge carriers inside the conductor. We assume that electron-electron and electron-phonon interactions can be neglected for the system in consideration and therefore the energy of the electrons is conserved. However, the distribution function does contain via the L(P)DOS the quantum mechanical phase coherence of the electron wave function throughout the system. Our effective distribution can be used to describe the electron distribution in phase-coherent diffusive conductors, if energy relaxation and dephasing can be neglected. To describe transport and noise in diffusive conductors one can also use the semi-classical Boltzmann-equation approach (see e. g. [30]). There, one introduces a distribution function which does not contain the quantum-mechanical phase-coherence but where energy relaxation processes can be modeled quite easily. However, the distribution function of this semi-classical approach can not be used for conductors where phase-coherence is essential.

At zero temperature we can replace the Fermi functions in Eq. (27) by step functions and get in linear response to the applied potentials

$$\langle I_{tip} \rangle = G(x) \{ V_{tip} - V_{eff}(x) \}, \quad (29)$$

where the conductance  $G(x) = (e^2/h) T_{ts}(x)$  has to be taken at the Fermi energy and

$$V_{eff}(x) = \sum_{\alpha} \frac{\nu(x, \alpha)}{\nu(x)} V_{\alpha}. \quad (30)$$

The same formula for the average current is also true for the case of arbitrary temperature provided that the

L(P)DOS,  $\nu(x, \alpha)$ , are independent of the energy in an energy interval  $\Delta E \approx kT$  around the Fermi-energy.

A particularly interesting setup is, when the tip is used as a voltage probe, i. e. we demand that on the average there is no net current flowing into the tip,  $\langle I_{tip} \rangle = 0$ . Similar experiments, also called scanning tunneling potentiometry, have initially been performed by Muralt and Pohl [41] and were later continued and refined by several groups [42–44]. From Eq. (29) we find that at zero temperature the voltage one has to apply at the tip to achieve the zero-current condition is exactly the effective voltage  $V_{eff}(x)$  defined in Eq. (30). The measured effective potential  $V_{eff}(x)$  should not be confused with the actual electrostatic potential  $U(x)$  inside the conductor. The injectivities  $\nu(x, \alpha)$  and the LDOS  $\nu(x)$  are determined by the equilibrium electrostatic potential  $U_{eq}(x)$  in the sample [16] and, therefore, also the measured effective potential  $V_{eff}(x)$  depends on the electrostatic potential. However, there is no direct relation between the measured potential and the actual electrostatic potential in the sample.

## B. Current fluctuations at the tip

We proceed by investigating the fluctuation-spectrum of the current at the tip. From Eq. (21) we get to the lowest order in the coupling parameter  $|t|$ ,

$$\begin{aligned} \langle (\Delta I_{tip})^2 \rangle &= 2 \int dE G(x) [f_{eff}(x) \{1 - f_{tip}(E)\} \\ &\quad + f_{tip}(E) \{1 - f_{eff}(x)\}] \end{aligned} \quad (31)$$

with the two-terminal conductance  $G(x)$  and the effective distribution function  $f_{eff}(x)$  as defined in Eq. (28). The fluctuations are therefore, as was the average current, determined by the effective distribution function. If we adjust the potential at the tip  $V_{tip}$  such that the average current at the tip vanishes, we get for the fluctuations

$$\langle (\Delta I_{tip})^2 \rangle = 4 \int dE G(x) \{1 - f_{tip}(E)\} f_{eff}(x). \quad (32)$$

In Eq. (31) the integral over energy extends from the bottom of the conduction band to infinity. At a temperature  $T$  and applied potential differences  $\Delta V$ , the relevant contribution to the current fluctuations comes from the integration over an energy range of about  $\Delta E \approx \max(e\Delta V, kT)$  around the Fermi-energy. If the LPDOS are nearly independent of energy in this energy range, we can evaluate the integral over products of Fermi functions and get for a potential  $V_{tip}$  at the tip and potentials  $V_{\alpha}$  at the massive contacts

$$\begin{aligned} \langle (\Delta I_{tip})^2 \rangle &= 2eG(x) \sum_{\alpha=1}^N |V_{\alpha} - V_{tip}| \\ &\quad \times \frac{\nu(x, \alpha)}{\nu(x)} \coth \left( \frac{e|V_{\alpha} - V_{tip}|}{2kT} \right). \end{aligned} \quad (33)$$

If we consider the case of a measurement on a wire with two contacts and choose  $V_{tip} = V_{eff}$  such that on average there is no current flowing into the tip, we get

$$\langle(\Delta I_{tip})^2\rangle = 2eG(x)\Delta V \frac{\nu(x,1)}{\nu(x)} \left(1 - \frac{\nu(x,1)}{\nu(x)}\right) \times \sum_{\alpha=1}^2 \coth\left(\frac{\nu(x,\alpha)}{\nu(x)} \frac{e\Delta V}{2kT}\right) \quad (34)$$

with  $\Delta V = V_1 - V_2$ . In the limit  $e\Delta V \ll kT$  this leads to

$$\langle(\Delta I_{tip})^2\rangle \approx 4G(x)kT + \frac{1}{3}eG(x)\Delta V \frac{e\Delta V}{kT} \frac{\nu(x,1)}{\nu(x)} \left(1 - \frac{\nu(x,1)}{\nu(x)}\right), \quad (35)$$

where we neglected corrections of order  $(e\Delta V/kT)^2$ . In this case the current fluctuations are due to thermal Johnson-Nyquist noise and a small correction which depends on the applied bias  $\Delta V$ .

As a next step we restrict ourselves to the case of zero temperature and sufficiently small differences in the applied potentials  $V_\alpha$  so that we are in the linear response regime. We are then dealing with pure shot-noise which is completely determined by the properties of the system (the scattering matrix) at the Fermi energy. For arbitrary potentials  $V_\alpha$  (though always close to the equilibrium value) we get from Eq. (31) for the current fluctuations at the tip

$$\langle(\Delta I_{tip})^2\rangle = 2eG(x) \sum_{\alpha} \frac{\nu(x,\alpha)}{\nu(x)} |V_\alpha - V_{tip}|. \quad (36)$$

The conductance, i. e. the densities of states and the coupling element  $t$  contained in it, have to be taken at the Fermi energy. This result shows that the fluctuations in the tip are just the addition of the fluctuations proportional to the conductances between the tip and the two massive contacts of the wire. This is not surprising, since, as is well known, the fluctuations of the current at a tunneling contact between two reservoirs are proportional to its conductance [21].

Eq. (36) is valid for arbitrary voltage configurations. Let us now choose the potential of the tip such that on average there is no net current flowing into the tip, i. e. we have to choose  $V_{tip} = V_{eff}(x)$  according to Eq. (30). Let us assume that the applied potentials at the sample are arranged in a way that  $V_\alpha < V_\beta$  for  $\alpha > \beta$  and let  $n$  be such, that  $V_\alpha > V_{eff}$  for  $\alpha \leq n$  and  $V_\alpha < V_{eff}$  for  $\alpha \geq n+1$ . The fluctuations at the tip can then be written in the form

$$\begin{aligned} \langle(\Delta I_{tip})^2\rangle &= 4eG(x) \sum_{\alpha=1}^n \frac{\nu(x,\alpha)}{\nu(x)} \{V_\alpha - V_{eff}(x)\} \\ &= 4eG(x) \sum_{\alpha=n+1}^N \frac{\nu(x,\alpha)}{\nu(x)} \{V_{eff}(x) - V_\alpha\}. \end{aligned} \quad (37)$$

For the case of measurements on a two terminal conductor as shown in Fig. 1, this formula reduces to

$$\langle(\Delta I_{tip})^2\rangle = 4eG(x)\Delta V \frac{\nu(x,1)}{\nu(x)} \left(1 - \frac{\nu(x,1)}{\nu(x)}\right). \quad (38)$$

with  $\Delta V = V_1 - V_2$ . This shows that at zero temperature  $\nu(x,1)/\nu(x)$  plays the role of the non-equilibrium distribution function.

### C. Voltage fluctuations at the tip

In the previous section we discussed the fluctuation spectrum of the current at the tip while we assumed that the potential at the tip is fixed and independent of time. Let us now investigate the experimental setup shown in Fig. 3, where the current at the tip is zero and we measure the fluctuation spectrum of the voltage using an infinite impedance voltmeter. If currents and voltages are related by the linear response formula, Eq. (22), the voltage fluctuation spectrum is directly related to the current fluctuation spectrum, Eq. (24). For the case of zero temperature, we can use the conductances from Eqs. (25) and (26) to get the fluctuation spectrum

$$\langle(\Delta V_{tip})^2\rangle = 4eR(x)\Delta V \frac{\nu(x,1)}{\nu(x)} \left(1 - \frac{\nu(x,1)}{\nu(x)}\right) \quad (39)$$

with  $R(x) = G(x)^{-1}$ . Results for the voltage and current fluctuations at finite temperature and in linear response to the applied potentials are presented in Appendix B. Next we will illustrate the main results of the previous section on some examples.

### D. Examples

The most simple example is a perfect ballistic conductor with one propagating channel. The local density of states as well as the injectivities are then independent of position. The injectivities from the left and right contacts are  $\nu_0 = 1/hv$  and the LDOS is  $2\nu_0$ . At zero temperature, this gives the position independent effective voltage  $V_{eff} = (V_1 + V_2)/2$  and from Eq. (38) the fluctuation spectrum

$$\langle(\Delta I_{tip})^2\rangle = 2eG_0\Delta V \frac{1}{2}, \quad (40)$$

with  $G_0 = (e^2/h)4\pi^2\nu_{tip}|t|^22\nu_0$  and  $\Delta V = V_1 - V_2$ . Note that a perfect conducting two terminal conductor shows no fluctuations of the currents at its contacts. The presence of the tip introduces shot noise into the system because in the presence of the tip electrons entering the system from let's say contact 1 have now the possibility to go either to contact 2 (what they do most of the time)



or to enter the tip (what they do with a probability proportional to  $|t|^2$ ). The fluctuations at the tip cause also the current at the massive contacts to fluctuate. At the massive contacts however, there is a considerable average current of the order of one, while the fluctuations are only of the order of  $|t|^2$ .

As a next step we introduce scattering in the wire. Let us assume that there is a scattering region described by a scattering matrix which leads to the transmission probability  $T$  and reflection probability  $R = 1 - T$  for the electrons. To the left of the scattering region the LDOS and the injectivities are [45]

$$\nu(x, 1) = \nu_0(2 - T + 2\sqrt{1 - T} \cos(2kx + \phi)), \quad (41)$$

$$\nu(x, 2) = \nu_0 T, \quad (42)$$

$$\nu(x) = 2\nu_0(1 + \sqrt{1 - T} \cos(2kx + \phi)), \quad (43)$$

where  $\phi$  is the phase acquired by reflected particles. Putting these densities into the fluctuation spectrum, Eq. (38), leads to

$$\langle(\Delta I_{tip})^2\rangle = 2eG_0\Delta VT \left(1 - \frac{T}{2} \frac{1}{1 + \sqrt{R} \cos(2kx + \phi)}\right). \quad (44)$$

As a function of the position  $x$  of the tip, the fluctuation spectrum oscillates with a period of half a Fermi wavelength. If we average this position dependent spectrum over one period we get

$$\langle(\Delta I_{tip})^2\rangle_{ave} = 2eG_0\Delta VT(1 - \sqrt{T}/2). \quad (45)$$

Averaging over the whole length of the conductor can mean to really move one single tip along the wire, always adjusting the electro-chemical potential such that there is zero average current into the tip and measuring the fluctuation spectrum. But it could also mean to attach very many tips (or electron absorbers) all along the wire, each one with its electro-chemical potential adjusted such that there is no net current flowing into it and neglecting the transmission of electrons from one tip to another ( $\propto |t|^4$ ). It is interesting to compare Eq. (45) to the fluctuations measured at contact 1 of an isolated (no tip present) wire [21],

$$\langle(\Delta I_1)^2\rangle = 2e \frac{e^2}{h} \Delta VT(1 - T). \quad (46)$$

Neglecting the interference of incoming and reflected waves in the local densities, i. e. setting  $\nu(x, 1) = \nu_0(2 - T)$  and  $\nu(x) = 2\nu_0$ , one gets from Eq. (38),  $\langle(\Delta I)^2\rangle \propto T(1 - T/2)$ .

The voltage fluctuations, Eq. (39), are in the phase-sensitive case, Eqs. (41)-(43), given by

$$\begin{aligned} \langle(\Delta V_{tip})^2\rangle &= 2eR_0\Delta V \frac{T}{1 + \sqrt{R} \cos(2kx + \phi)} \\ &\times \left(1 - \frac{T}{2} \frac{1}{1 + \sqrt{R} \cos(2kx + \phi)}\right) \end{aligned} \quad (47)$$

with  $R_0 = G_0^{-1}$ . The current- and voltage-fluctuations together with the effective potential  $V_{eff}(x)$  are shown in Fig. 4.

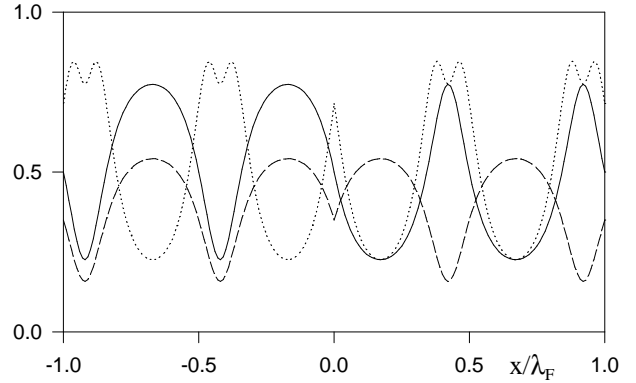


FIG. 4. Fluctuation spectra and effective voltage measured along a ballistic wire with a  $\delta$  barrier at  $x = 0$  leading to a transmission probability  $T = 0.7$ . The solid line is  $(V_{eff} - V_2)/\Delta V$ , the dashed line gives the current fluctuations  $\langle(\Delta I_{tip})^2\rangle$  in units of  $2eG_0\Delta V$ , and the dotted line shows the voltage fluctuations  $\langle(\Delta V_{tip})^2\rangle$  in units of  $2eR_0\Delta V$ .

An interesting system containing very many scatterers is a metallic diffusive wire of length  $L$  and width  $W$  which is at its ends attached to two ideal leads. The elastic mean free path is  $l$ . We assume that  $l \ll W \ll L$  so that the diffusion in the wire can be treated to be effectively one-dimensional. Furthermore we assume that there is no inelastic scattering inside the conductor. For a given wire, i. e. a given disorder configuration, the exact LPDOS are given in terms of Green's functions by Eqs. (8) and (12). Here, we are only interested in the quantities averaged over many different disorder configurations. While the ballistic conductor with one single barrier could serve as a model to illustrate what is measured in the neighborhood of an impurity, the ensemble averaged quantities correspond to the average of many measurements on a diffusive conductor at different locations over a spatial range of about an elastic mean free path. To average expressions given as products of retarded and advanced Green's functions we use the diagram technique [46]. For the injectivities we have to average the product of retarded and advanced Green's functions between the coupling point of the tunneling tip and two points on the surface between the diffusive region and the ideal leads. For the averaged quantities we get (see appendix A for details)

$$\nu(x, 1) = \nu_0(L - x)/L \quad \text{and} \quad \nu(x, 2) = \nu_0 x/L \quad (48)$$

with the two-dimensional density of states  $\nu_0 = m^*/2\pi\hbar^2$ .

At zero-temperature, the effective voltage measured along the wire gives averaged over the ensemble the classical linear voltage drop,  $V_{eff}(x) = V_2 + \Delta V(L - x)/L$ ,



and the parabolic behavior of the current fluctuation spectrum as a function of the tip position,

$$\langle(\Delta I_{tip})^2\rangle = 2eG_0\Delta V \frac{x(L-x)}{L^2}. \quad (49)$$

As in the case of the ballistic conductor with barrier, we can average the fluctuation spectrum over the hole length of the diffusive region and get

$$\langle\langle\Delta I_{tip}\rangle^2\rangle = 2eG_0\Delta V \frac{1}{6}. \quad (50)$$

This is exactly 1/3 of the fluctuations that would be measured at a tip probing a perfect ballistic conductor, Eq. (40). It is very well known, that the fluctuations measured at a contact of a diffusive wire are suppressed by a factor of 1/3 with respect to full shot noise (see e. g. Refs. [47,48,30]). Therefore, it is tempting to say that the fluctuations at the tip reflect the fluctuations of the current inside the isolated (without the tip) wire. Nevertheless, the presence of the tip does change the system since it offers the electrons another possibility (even though a very weak one, proportional to  $|t|^2$ ) where to travel. Therefore the tip introduces additional fluctuations in the system, as we saw for example when the tip couples to a perfect ballistic conductor.

If we neglect the energy dependence of the injectivities, Eq. (48), (temperature and applied bias  $\Delta V = V_1 - V_2$  sufficiently small) we can use Eq. (34) to illustrate the crossover from the position dependent shot-noise at zero temperature to the position independent thermal noise at elevated temperatures. For the metallic diffusive wire we get

$$\langle(\Delta I_{tip})^2\rangle = 2eG_0\Delta V \frac{(L-x)x}{L^2} \times \left\{ \coth\left(\frac{L-x}{L} \frac{e\Delta V}{2kT}\right) + \coth\left(\frac{x}{L} \frac{e\Delta V}{2kT}\right) \right\}. \quad (51)$$

This crossover is shown in Fig. 5. In Fig. 6, we plot for fixed temperature  $T$  the voltage dependence of the fluctuation spectrum if the tip is placed at different positions along the wire.

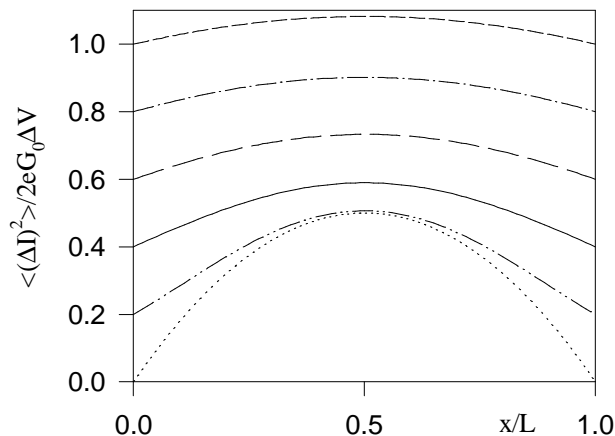


FIG. 5. The current fluctuation spectrum along a diffusive wire from 0 to  $L$  for different temperatures. The temperature range  $kT$  is from 0 to  $0.5e\Delta V$  in steps of  $0.1e\Delta V$ . Lower temperatures correspond to lower curves.

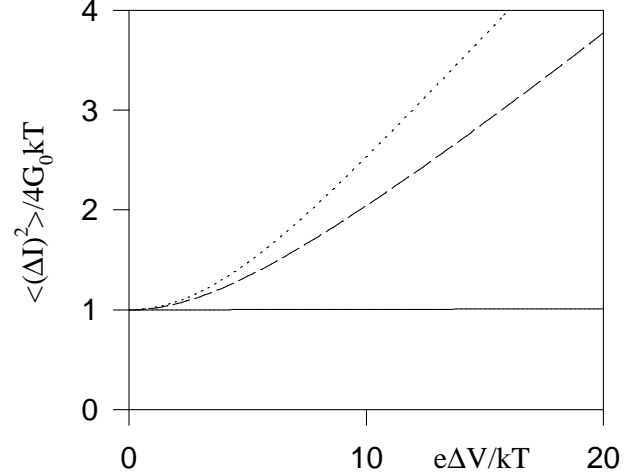


FIG. 6. Voltage dependence of the current fluctuation spectrum for fixed temperature. The three curves correspond to different positions of the tip. The tip is placed at  $x = 0$  (solid line),  $x = L/4$  (dashed line) and  $x = L/2$  (dotted line).

## V. CURRENT CORRELATIONS AT TWO TUNNELING PROBES

In this Section we make predictions for the cross-correlation of the currents at two contacts. Recently, two groups succeeded in measuring the correlation spectrum of the current at two different contacts of a multi-probe sample [33,34]. We consider a mesoscopic wire with two

$$\begin{aligned} \langle \Delta I_{tip1} \Delta I_{tip2} \rangle &= 2e \frac{e^2}{h} 4\pi^2 \nu_{tip1} \nu_{tip2} |t|^4 \\ &\times \left[ 2\text{Re}\{2\pi\nu(x, x', 1)2\pi\nu(x', x, 2)\}|V_1 - V_2| - 2\text{Re}\{G(x, x')G(x', x)\}|V_3 - V_4| \right. \\ &\left. + \sum_{\delta=1,2} 2\text{Im}\{2\pi\nu(x, x', \delta)G(x', x)\}|V_3 - V_\delta| + \sum_{\delta=1,2} 2\text{Im}\{2\pi\nu(x', x, \delta)G(x, x')\}|V_4 - V_\delta| \right]. \end{aligned} \quad (52)$$

We now want to illustrate this result for some specific voltage configurations. One particularly interesting case is the exchange experiment proposed in [20] for arbitrary four terminal conductors. Such an experiment has been performed recently by Liu *et al.* [36] on a ballistic conductor. Theoretical predictions have been made by Blanter and Büttiker [29] and by Sukhorukov and Loss [30] for metallic diffusive conductors and by van Langen and Büttiker [31] for chaotic cavities. To identify the exchange contribution in the noise spectrum one performs three successive experiments. In the first two experiments, called experiment A and B, current is injected into the system only through one single contact respectively. In the third experiment, called experiment C, current is injected through both contacts simultaneously. The correlation spectrum is always measured at the same two terminals in all three experiments. The current injection is achieved by rising the potential of the respective contact to the elevated value  $V_h$  keeping the other ones at the equilibrium value  $V_0$ . In principle, one is free to choose through which contacts current should be injected and at which two contacts the correlations should be measured. In our system we have an obvious asymmetry between the two massive contacts 1 and 2 of the wire and the two tunneling contacts 3 and 4. In equation (52) we decided to look at the current correlations at the two tunneling tips. The current correlations at the two massive contacts will be discussed later. Still we can decide through which contacts we want to inject the current, either through the massive contacts or through the tunneling contacts. Experimentally, the first case (contacts for current measurement and current injection different) should be easier to achieve. For both cases we can rewrite Eq. (52) in the form

$$\langle \Delta I_{tip1} \Delta I_{tip2} \rangle = -4e \frac{e^2}{h} 16\pi^4 \nu_{tip1} \nu_{tip2} |t|^4 V S_{A,B,C}^{m,t}. \quad (53)$$

Here, the upper index  $m$  indicates that the current is injected through the massive contacts whereas the index  $t$  means that current is injected through the tips.

tips weakly coupled at points  $x$  and  $x'$  as shown in figure 2. For the following discussion, we consider the zero temperature limit and the linear response regime with respect to the applied potentials. According to Eq. (21) the correlation of the currents at the two tips  $\langle \Delta I_{tip1} \Delta I_{tip2} \rangle$  is a function of all possible voltage differences  $|V_\alpha - V_\beta|$ . Using the two point density of states, Eq. (15), we find

The lower indices distinguish the three experiments and  $V = V_h - V_0$ .

### A. Current injection through the massive contacts

First we consider the case of current injection through the massive contacts. Performing the three above mentioned experiments leads to the following voltage configurations: for experiment A,  $V_1 = V_h$ , for experiment B,  $V_2 = V_h$  and for experiment C,  $V_1 = V_2 = V_h$ . All other potentials are held at the equilibrium value  $V_0$ . We get

$$S_A^m = |\nu(x, x', 1)|^2, \quad (54)$$

$$S_B^m = |\nu(x, x', 2)|^2, \quad (55)$$

$$\begin{aligned} S_C^m &= \frac{1}{4\pi^2} |G(x, x') - G^\dagger(x, x')|^2 \\ &= |\nu(x, x', 1) + \nu(x, x', 2)|^2 \\ &= S_A^m + S_B^m + 2\text{Re}\{\nu(x, x', 1)\nu(x', x, 2)\}. \end{aligned} \quad (56)$$

The current-correlations are for all three experiments determined by the spatially non-diagonal injectivities, Eq. (15), which are also given as products of wave functions. Equations which express the current correlations in terms of wave functions can be found in [37], Eqs. (8)-(11). It is not surprising that the result for experiment A with current injected through contact 1 depends only on the (non-diagonal) injectivity of contact 1, while experiment B with the current injected through contact 2 depends only on the (non-diagonal) injectivity of contact 2. One sees also at once, that the result for experiment C is in general not only the addition of experiments A and B but contains the *exchange* term

$$\begin{aligned} S_X^m &= S_C^m - S_A^m - S_B^m \\ &= 2\text{Re}\{\nu(x, x', 1)\nu(x', x, 2)\}. \end{aligned} \quad (57)$$

This exchange term is due to the quantum mechanical *indistinguishability* of the charge carriers. In the following we investigate for which systems or under which conditions this term vanishes or becomes important. The

question if phase-coherence is necessary for the existence of the exchange term will also be addressed below.

## B. Examples

We investigate Eqs. (54)-(56) in more detail for three examples. The most simple system one can think of is a perfect ballistic one channel conductor. The two scattering states at the Fermi-energy are then simple plain waves so that the non-diagonal injectivities at the Fermi-energy are

$$\nu(x, x', \alpha) = \frac{1}{\hbar v} e^{ik_\alpha(x-x')}, \quad (58)$$

with  $k_1 = -k_2 = m^*v/\hbar$  and the Fermi velocity  $v = \sqrt{2E_F}/m^*$ . That means that the correlations in experiments A and B are independent of the distance  $d = x - x'$  of the tips. However, the correlations of experiment C and therefore the exchange contribution, Eq. (57), depend on this distance. They oscillate with the period of half a Fermi-wavelength,

$$S_C^m = 4 \frac{1}{\hbar^2 v^2} \cos^2(kd). \quad (59)$$

Moving one of the tips over the distance of half a Fermi-wavelength and averaging the results, gives the averaged spectrum

$$\langle S_C^m \rangle = 2 \frac{1}{\hbar^2 v^2} = S_A + S_B \quad (60)$$

which is again independent of the distance between the tips. The exchange term averages to zero. Moving the tips along the wire means in this case averaging over the phase of the wave function. Therefore, for this type of conductors (applies also to perfect ballistic multi-channel conductors) phase coherence is crucial for the existence of an exchange term. A perfect ballistic (multichannel) conductor exhibits no fluctuations at zero temperature, and thus the result found above might represent a very particular situation. Thus now we introduce scattering in the wire, i. e. we introduce a barrier of transmission probability  $T$  in the middle of the wire. This changes the noise properties of the wire in a qualitative way: due to the possibility of backscattering the current in the massive contact of the wire fluctuates already without a tip being present. Now, we place tip 1 to the left of the barrier and tip 2 to the right of the barrier. We assume one propagating channel on each side of the barrier so that the barrier is described by a  $2 \times 2$  matrix, which determines the scattering states on the two sides. We find

$$S_A^m = 2\nu_0^2 T [1 - T/2 - a(2kx - \phi)], \quad (61)$$

$$S_B^m = 2\nu_0^2 T [1 - T/2 + a(2kx' + \phi)], \quad (62)$$

$$\begin{aligned} S_C^m &= 2\nu_0^2 T \times 2 \cos^2\{k(x - x') - \phi\} \\ &= 2\nu_0^2 T - 2\nu_0^2 T \cos\{2k(x - x') - 2\phi\}, \end{aligned} \quad (63)$$

with  $a(z) = \sqrt{1-T} \sin(z - \phi_a)$ . Here,  $\nu_0 = 1/\hbar v$  is the density of scattering states,  $\phi$  is the phase acquired by an electron traveling through the barrier and  $\phi_a$  is the phase which takes into account a possible asymmetry of the barrier [45]. The spectrum of experiments A and B in which current is injected only through one single contact depends only on the position of the tip at that side of the barrier where current is injected. Comparison of the spectrum of experiment C for the pure ballistic wire Eq. (59), with that for a wire with a barrier shows that these spectra differ only in that the spectrum of the wire with a scatterer is multiplied by the transmission probability  $T$  and in that it depends on  $\phi$ , the phase acquired by transmitted electrons. Again, we find a non-vanishing exchange term  $S_X^m = S_C^m - S_A^m - S_B^m$ . Moving the tips on both sides of the barrier over a Fermi wavelength does not cause the exchange term to vanish, but leads to

$$S_X^m = -2\nu_0^2 T(1 - T). \quad (64)$$

Thus elastic scattering has established a correlation in the exchange term which does not vanish upon averaging.

It is an interesting question whether an exchange term exists also for measurements on diffusive conductors or not. Starting from exact quantum mechanical expressions for the correlation spectrum and performing a disorder average, Blanter and Büttiker [29] found a non-vanishing exchange term for cross shaped diffusive conductors. An exchange term for diffusive four-terminal conductors of arbitrary shape was found by Sukhorukov and Loss [30] using a semi-classical Maxwell-Boltzmann equation approach which does not contain the quantum mechanical phase coherence of the system. In our approach, we start with the quantum mechanical expressions for the non-diagonal injectivities, Eq. (15) and average these quantities over many different disorder configurations. We assume the conductor to be a long and narrow strip as discussed in Section IV, and, similarly to Ref. [29] use the diagram technique to average products of Green's functions. Performing the averages leads to the following expressions for the noise spectra [37] (details see appendix A)

$$S_A^m = \frac{S_C}{2} \frac{(L - x)^2 + (L - x')^2 + p(x, x')}{L^2}, \quad (65)$$

$$S_B^m = \frac{S_C}{2} \frac{x^2 + (x')^2 + p(x, x')}{L^2}, \quad (66)$$

$$S_C^m = \frac{(m^*)^2}{(\pi\hbar)^2 N} \frac{L}{l} \frac{x(L - x')}{L^2}, \quad (67)$$

where  $p(x, x') = 1/3[(x - x')^2 - 2x'(L - x)]$ . From these results we can extract the relative strength of the exchange term  $S_X^m$  to be

$$\frac{S_X^m}{S_C^m} = \frac{1}{L^2} [x(L - x) + x'(L - x') - p(x, x')]. \quad (68)$$

The exchange term always has the same sign as the spectra  $S_A^m$  and  $S_B^m$ , i. e. it enhances the correlation spectrum  $S_C^m$  over the pure addition  $S_A^m + S_B^m$ . An enhancement of the current correlations due to the exchange term was also predicted for a chaotic cavity with four tunneling contacts [31]. To illustrate the exchange term further, we assume a specific configuration of the two tips: we place the two tips symmetrically around the center  $L/2$  of the wire. One is placed a distance  $d/2$  to the left of the center, the other one the same distance  $d/2$  to the right. The strength of the exchange term as a function of the distance  $d$  between the tips is then

$$\frac{S_X^m}{S_C^m} = \frac{1}{3} \left( 2 + \frac{d}{L} - 2 \left( \frac{d}{L} \right)^2 \right). \quad (69)$$

This function reaches its maximum not when the tips are closest (a limit where our approximations for the disorder average are not anymore valid), but at the finite distance  $d = L/4$ . It's maximal value is  $(S_X^m/S_C^m)_{max} = 17/24$ . At first sight, it might seem quite surprising to have the maximal correlations when the tips are separated by  $d = L/4$ . This can be understood if one considers that the strength of the correlations is determined by scattering between all four contacts and, therefore, not only the distance in between the tips counts, but also the distances from the coupling points of the tips to the massive contacts of the wire. Moving the tips away from the center of the wire increases the distance in between them, but decreases the distances to the massive contacts. The correlations are then determined by an interplay of contributions from the differing types of possible electron paths. This example again demonstrates that in the presence of elastic scattering, the exchange contribution survives ensemble averaging. This is consistent with the results of Refs. [29,30].

Let us consider as a last example a system consisting of a quantum dot in the quantum Hall regime, to which two leads are attached via quantum point contacts, Fig. 7.

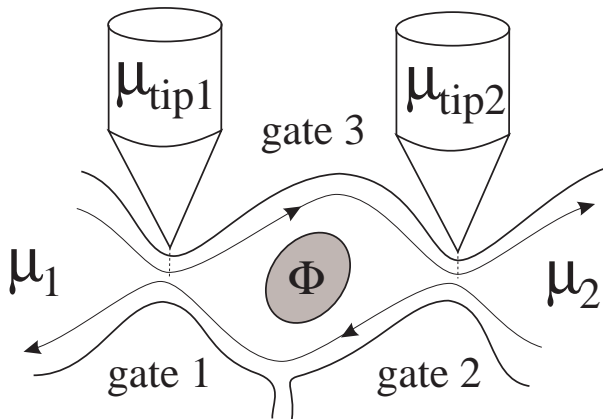


FIG. 7. Mesoscopic ring in the quantum Hall regime with one propagating edge channel. An additional magnetic flux penetrates the center of the ring which is not accessible to the electrons. Two tunneling tips are placed at the center of the point contacts which connect the ring to two electron reservoirs.

A very similar geometry was investigated in Ref. [27]. We re-consider this example since the two-point injectivity Eq. (15) provides a particularly clear formulation and also to use this opportunity to correct an algebraic mistake in one of the results of Ref. [27]. The sample is penetrated by a quantizing magnetic field which leads to the formation of edge channels. The voltages at the gates forming the two point contacts are chosen such that there is exactly one propagating edge channel which is perfectly transmitted through the sample whereas all other edge channels are completely reflected at the point contacts. In addition to the strong magnetic field there is an additional field present only in the center of the dot. The additional field is characterized by its flux  $\Phi$  through the dot. Since there is no backscattering at all of electrons in the propagating edge channel, the transmission probability of the system is independent of the flux  $\Phi$ . For the same reason transmission from one tip to the other or to the massive contacts is also independent of  $\Phi$ . Without backscattering there is no closed electron path encircling the flux. Now we place two tunneling tips in the middle of the two point contacts 1 and 2. There, the tips should couple equally well to the left going and to the right going edge channel. We are interested if the correlation of the currents at the two tips depends on  $\Phi$ . To answer this question we only need to know the scattering wave functions at the two coupling points. Let us denote the amplitude of the scattering state incoming from the left contact at the left point contact by  $\psi_1(1)$  and the one incoming from the right contact at the right point contact by  $\psi_2(2)$ . The electron state  $\psi_1$  acquires now on its way from the left to the right point contact an additional phase  $\phi_1$  due to its propagation and the presence of the background quantizing magnetic field. In addition, it's phase is changed by  $\theta/2$  due to the flux  $\Phi$ . Therefore, we have  $\psi_1(2) = \psi_1(1)e^{i\phi_1}e^{i\theta/2}$ . Similarly, we have  $\psi_2(1) = \psi_2(2)e^{i\phi_2}e^{i\theta/2}$ . As before,  $\phi_2$  is the phase acquired due to propagation and the presence of the quantizing field and  $\theta/2$  is due to the flux  $\Phi$ . For all closed paths encircling the flux one must have

$$\oint_S \mathbf{A} ds = 2\pi \frac{\Phi}{\Phi_0} = \theta. \quad (70)$$

We chose a gauge such that the phase  $\theta$  is divided into equal parts on the upper and the lower half circle along the edge of the dot. Putting these wave functions into the expression for the current correlations at the tips, Eq. (56), yields

$$S_C^m \propto 2 + 2 \cos\{(\phi_1 + \phi_2) + \theta\} \quad (71)$$

i. e. the exchange term is  $S_X^m = 2 \cos\{(\phi_1 + \phi_2) + \theta\}$ . (we

have used  $|\psi_1(1)|^2 = |\psi_2(2)|^2 = 1$ ). We see that the correlation spectrum in fact depends periodically on the flux and the period is  $\Phi_0$ . The measurement of the correlation spectrum thus allows to get information about the flux  $\Phi_0$ . This result corrects Eq. (15) of Ref. [27] where the periodicity of the correlation spectrum was found to be only  $\Phi_0/2$ . We remark that the exchange term depends on the phases  $\phi_1$  and  $\phi_2$  in a similar simple way as the exchange term of the pure ballistic wire. Again, moving the tips by the distance of a Fermi wavelength will lead to a vanishing exchange term. Furthermore this example shows that a cross-correlation can be sensitive to an Aharonov-Bohm flux even for a conductor (which in the absence of the tips) exhibits no Aharonov-Bohm effect. However, the situation discussed here and in Ref. [27] does not conclusively show that Aharonov-Bohm effects in second order correlations are possible even if there is no second order Aharonov-Bohm effect. If the conductance is measured in the presence of the two tips, then the weak scattering caused by the tips, which must after all couple to both edge states, leads to an Aharonov-Bohm effect, which is of the same magnitude (fourth order in the tunneling amplitudes) as the fourth order interference effect given by the current-current correlation.

### C. Current injection through the tips

We now consider slightly modified arrangements: instead of injecting the current through the massive contacts, we inject the current through the tips and measure simultaneously the correlations of the currents at the tips. The voltage configurations for the three experiments of this type are then for experiment A,  $V_3 = V_h$ , for experiment B,  $V_4 = V_h$  and for experiment C,  $V_3 = V_4 = V_h$ . All other potentials are held at the equilibrium value  $V_0$ . The correlation spectrum for experiment C is the same as the spectrum of experiment C with the current injected through the massive contacts since the spectrum depends only on the absolute value of voltage differences and not on the sign. Experiments A and B are, however, different from the respective experiments with current injection through the massive contacts. The quantities  $S_{A,B,C}^t$  which have to be used in Eq. (53) are

$$S_A^t = \frac{1}{4\pi^2} |G(x', x)|^2, \quad (72)$$

$$S_B^t = \frac{1}{4\pi^2} |G(x, x')|^2, \quad (73)$$

$$\begin{aligned} S_C^t &= \frac{1}{4\pi^2} |G(x, x') - G^\dagger(x, x')|^2 \\ &= S_A^t + S_B^t - \frac{1}{2\pi^2} \text{Re}\{G(x, x')G(x', x)\}, \end{aligned} \quad (74)$$

Since the potentials of both massive contacts are always held at the same potential, the equilibrium potential  $V_0$ , the correlation spectra do not show any dependence on

the (non-diagonal) injectivities of these two contacts separately. The wire acts as an effective one terminal conductor and all that enters in Eqs. (72)-(74) is the Green's function of the wire representing the total (non-diagonal) density of states of the wire. But as in the experiments discussed in the previous section an exchange term appears in general. To investigate this exchange term further we evaluate it for the example systems used before.

For a ballistic wire the result is qualitatively similar to the one found by current injection through the tunneling contacts. A qualitative change occurs for the wire with a barrier and in the case of a metallic diffusive wire. Let us first consider the ballistic wire with the barrier. In contrast to the experiments where current is injected through the massive contacts, the averaged exchange term does vanish when current is injected through the tips. Averaging means to move both tips over distances longer than a Fermi wavelength and average the measured spectra. For a metallic diffusive conductor it is easily seen that the exchange term vanishes. The average over disorder of a product of two retarded Green's functions is exponentially small. This is in remarkable contrast to the behavior of the exchange term in the experiments with current injection through the massive contacts. It is due to the fact, that the spectrum of experiments A and B changed while experiment C is the same as for current injection through massive contacts.

We can draw the following conclusions from this Section: For all the situations investigated here, we could identify an exchange contribution to the cross-correlation. In the case of a pure ballistic wire, the exchange contribution is a purely quantum mechanical effect which vanishes when averaging is performed (by moving the tip and averaging the results). As soon as some elastic scattering is present, as in the wire with a barrier, or in a metallic diffusive wire, the exchange term, in addition to a purely quantum mechanical contribution, also contains a "classical" contribution which survives ensemble averaging. This situation is thus reminiscent of the conductance of a mesoscopic sample which consists of a classical (Drude like) conductance and a small quantum mechanical sample specific contribution known as universal conductance fluctuation.

## VI. CURRENT CORRELATION AT THE MASSIVE CONTACTS

Until now we were only interested in the correlation of the currents at the tunneling tips. We saw that in the case of current injection through the massive contacts the correlations depend on non-diagonal partial densities of states, namely the non-diagonal injectivities of the massive contacts. There is still another partial density of states, the emissivities, which did not yet appear in the expressions for the correlation spectra. Emissivity and injectivity are related to each other by the symmetry relation, Eq. (13). The correlations of the currents at the tips

were determined by the transport properties of electrons injected through the massive contacts and transmitted to the tips. Therefore only the non-diagonal injectivities of the massive contacts appeared in the equations for the current correlations at the tips. If one investigates the correlation spectrum at the massive contacts one expects that it depends on the non-diagonal emissivities of these contacts. Clearly, if we also inject the current through the massive contacts, the correlation of the current in the massive contacts is to first order only determined by the wire with its two contacts and the presence of the two tips does not play a role at all. In this case, the correlation/fluctuation spectra are just the ones known for two probe conductors [21].

Consider the case, when current is injected through the tips. We investigate the experiments A:  $V_3 = V_h$ , B:  $V_4 = V_h$  and C:  $V_3 = V_4 = V_h$ . All other potentials are, as before, kept at  $V_0$ . The correlations can then be written in the form

$$\langle \Delta I_1 \Delta I_2 \rangle = -2e \frac{e^2}{h} 16\pi^4 |t|^4 eV S_{A,B,C} \quad (75)$$

with

$$S_A = \nu(1, x) \nu(2, x) \nu_{tip1}^2, \quad (76)$$

$$S_B = \nu(1, x') \nu(2, x') \nu_{tip2}^2, \quad (77)$$

$$S_C = \nu(1, x) \nu(2, x) \nu_{tip1}^2 + \nu(1, x') \nu(2, x') \nu_{tip2}^2 + 2\text{Re}\{\nu(1, x, x') \nu(2, x', x)\} \nu_{tip1} \nu_{tip2} \quad (78)$$

$$= S_A + S_B + 2\nu_{tip1} \nu_{tip2} \text{Re}\{\nu(1, x, x') \nu(2, x', x)\}. \quad (79)$$

The expressions for experiments A and B are products of the transmission probabilities from tip 1 resp. tip 2 into the two massive contacts of the wire, e. g. the transmission probability from tip 1 into contact 1 of the wire is  $T_{1,tip1} = 4\pi^2 \nu(1, x) |t|^2 \nu_{tip1}$  according to Eq. (26). The two spectra where current is only injected into the system through one single contact do not at all depend on the presence of the second tip. They depend only on the local emissivities of the massive contacts at the coupling point of the tip through which the current is injected. The correlation spectrum of experiment C where current is injected through both tips is sensitive to the non-diagonal emissivities of the massive contacts. In fact, the exchange contribution is

$$S_X = 2\nu_{tip1} \nu_{tip2} \text{Re}\{\nu(1, x, x') \nu(2, x', x)\} \quad (80)$$

This result again demonstrates the key role played by the the two point injectivity in cross-correlation spectra.

## VII. DISCUSSION

We have shown that the current fluctuation and correlation spectra measured at tunneling contacts on multi-probe conductors are related to local partial densities of states and to spatially non-diagonal (two point) densities

of states. The general expressions are illustrated for various examples, like perfect ballistic conductors, ballistic conductors with a barrier, metallic diffusive wires and mesoscopic rings in a magnetic field.

In particular, we found that the current fluctuations at a single tunneling tip are determined by an *effective local distribution function*  $f_{eff}(x)$ . This distribution function is given in terms of local partial densities of states, the injectivities of the contacts of the sample,  $f_{eff}(x) = \sum_{\alpha} (\nu(x, \alpha) / \nu(x)) f_{\alpha}(E)$ . It gives the local non-equilibrium distribution of charge carriers in a conductor. In the semi-classical Boltzmann-equation approach one relates the current fluctuations to local distribution functions. These distribution functions are solutions to the Boltzmann-equation with proper boundary conditions. They do not contain the quantum mechanical phase coherence of an electron state entering through contact  $\alpha$  and traveling to the point  $x$  in the conductor, whereas this information is included via the densities of states in our distribution function  $f_{eff}(x)$ . Our discussion bridges therefore at least to some extent the gap between quantum mechanical discussions of shot noise and purely classical treatments of current fluctuations. The effects of the phase coherence on the fluctuation spectrum is illustrated for measurements on a ballistic conductor with a barrier. This example is also useful to get a qualitative impression on how the noise spectrum looks like in the neighborhood of an impurity. We evaluate the general formula for the fluctuations at the tip also for the case of measurements on a metallic diffusive wire in the ensemble average.

The second part of this work treats the current correlations in two tunneling contacts. The correlations are determined by newly defined spatially non-diagonal and non-local densities of states. We used the exchange experiment [20] to investigate the magnitude of the exchange term in a four terminal configuration containing two tunneling tips. If current is injected through the massive contacts of the sample, the correlation spectrum at the tips is given by the spatially non-diagonal injectivities  $\nu(x, x', \alpha)$ . If current is injected through the tips, the correlation spectrum at the massive contacts is given by the non-diagonal emissivities  $\nu(\alpha, x, x')$ . An exchange term with a magnitude of the order of the total correlations was found for ballistic conductors and ballistic conductors with a barrier. The correlations are always negative while the exchange term can have either sign, depending on the positions of the tips. This can lead to a complete suppression of the correlations for certain tip positions. Even for the case of measurements on metallic diffusive conductors an exchange term exists, and it's magnitude can be as high as 70 % of the total correlations. In the average over the disorder configurations, the exchange term is always negative and therefore enhances the correlations. For the example of a mesoscopic ring penetrated by a magnetic flux we showed, that the current correlations measured in the tips can show a flux

dependence even though the conductances through the ring do not depend on the flux.

Clearly, the experiments proposed here, if carried out, would permit an unprecedented, detailed microscopic view of shot noise in mesoscopic conductors.

This work was supported by the Swiss National Science Foundation.

## APPENDIX A: ENSEMBLE AVERAGES FOR DIFFUSIVE WIRES

We consider a two-dimensional metallic diffusive wire of length  $L$  and width  $W$  with  $L \gg W$ . The elastic mean free path is  $l \ll W$ . Then the diffusion can be treated to be effectively one-dimensional. The diffusive wire is at its ends connected via a coupling matrix  $\Gamma_\alpha$  to two semi-infinite ideal leads.

### 1. Ensemble averaged injectivity

We are looking for the disorder average of the injectivity of contact  $\alpha$  at a point  $r = (x, y)$  inside the diffusive region, Eq. (8). We have to find the average of

$$\nu(r, \alpha) = \int_{S_\alpha} dy_1 dy_2 G(r, r_1) \Gamma_\alpha(y_1, y_2) G^\dagger(r_2, r). \quad (\text{A1})$$

Here, the integrals are over the surface between contact  $\alpha$  and the diffusive region. The coupling matrix  $\Gamma_\alpha(y, y')$  is independent of the disorder configuration inside the wire. The disorder average of Eq. (A1) is then

$$\langle \nu(r, \alpha) \rangle = \int_{S_\alpha} dy_1 dy_2 \Gamma_\alpha(y_1, y_2) \times \int dr_a S(r, r_a) \langle G(r_a, r_1) \rangle \langle G^\dagger(r_2, r_a) \rangle. \quad (\text{A2})$$

The integral over the intermediate point  $r_a$  is over the entire diffusive region. The propagator

$$S(r, r') = \frac{1}{D\tau WL} \begin{cases} x'(L-x) & x > x' \\ x(L-x') & x < x' \end{cases} \quad (\text{A3})$$

with the diffusion coefficient  $D = v_F l / 2$  and the elastic lifetime  $\tau = l / v_F$  describes the diffusion from the point  $r$  to  $r'$ . In particular, this propagation is independent of the  $y$  coordinate provided that  $|x - x'| \gg l$ . The exponentially decaying averaged Green's functions can be approximated as

$$\langle G(r, r') \rangle = -\frac{im^*}{\hbar p_F} \exp \left[ \left( ip_F - \frac{1}{2l} \right) |x - x'| \right] \delta(y - y'). \quad (\text{A4})$$

Performing the integrals and using  $\int dy_\alpha \Gamma_\alpha(y_\alpha, y_\alpha) = v_F N_\alpha / 4\pi$  ( $N_\alpha = k_F W$  is the number of open channels in contact  $\alpha$ ) then gives

$$\langle \nu(r, 1) \rangle = \nu_0 \frac{L-x}{L}, \quad (\text{A5})$$

and

$$\langle \nu(r, 2) \rangle = \nu_0 \frac{x}{L}. \quad (\text{A6})$$

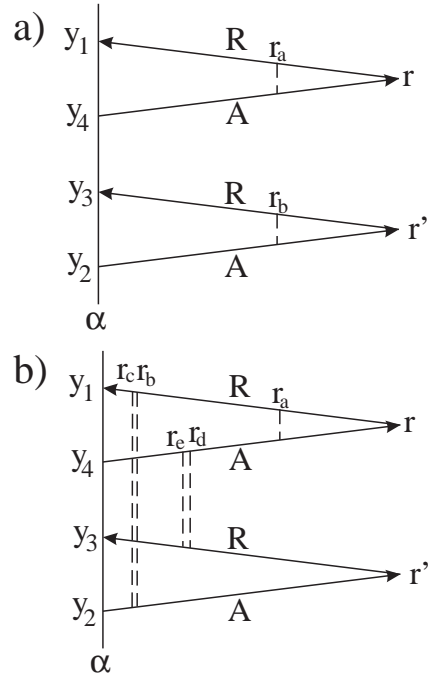
Here, we used the two dimensional density of states  $\nu_0 = m^* / 2\pi \hbar^2$ . The injectivities are linearly decaying, respectively, growing as functions of the position  $x$  along the wire. They are independent of the transverse coordinate  $y$ .

### 2. Ensemble averaged non-diagonal injectivity

In Section V we found that the current correlations were proportional to absolute squares of non-diagonal injectivities,

$$|\nu(r, r', \alpha)|^2 = \int_{S_\alpha} dy_1 dy_2 dy_3 dy_4 \Gamma_\alpha(y_1, y_2) \Gamma_\alpha(y_3, y_4) \times G(r, r_1) G^\dagger(r_2, r') G(r', r_3) G^\dagger(r_4, r). \quad (\text{A7})$$

Now, we are interested in the average of this quantity over many different disordered wires. Again, the  $\Gamma$ 's are independent of the impurity configuration inside the wire, so that it remains to find the average of the product of four Green's functions. The averaged quantity has contributions from diagrams with two, three and four diffusion propagators, as shown in figure 8.





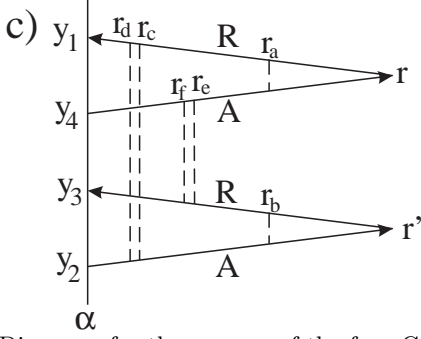


FIG. 8. Diagrams for the average of the four Greens functions using (a) two diffusions, (b) three diffusons and (c) four diffusons. A single dashed line indicates the propagation with the propagator  $S(r, r')$  and two neighboring dashed lines indicate propagation with  $P(r, r')$ .

It is interesting to compare these diagrams for the two-point injectivity with the ones given by Blanter and one of the authors [29] which apply in a discussion of the shot noise at the contacts of metallic diffusive conductors. It turns out that diagrams with two and three diffusons are small as  $l/L$ , respectively  $(l/L)^2$ , compared to the diagram with four diffusons and are therefore neglected. From the diagram with four diffusion propagators we get

$$\begin{aligned} \langle |\nu(r, r', \alpha)|^2 \rangle &= \int_{S_\alpha} dy_1 dy_2 dy_3 dy_4 \Gamma_\alpha(y_1, y_2) \Gamma_\alpha(y_3, y_4) \\ &\times \int dr_a dr_b dr_c dr_d dr_e dr_f S(r, r_a) S(r', r_b) \\ &\times P(r_c, r_d) P(r_e, r_f) \langle G(r_d, r_1) \rangle \langle G^\dagger(r_2, r_d) \rangle \\ &\times \langle G(r_f, r_3) \rangle \langle G^\dagger(r_4, r_f) \rangle F(r_b, r_c, r_a, r_e). \end{aligned} \quad (\text{A8})$$

Here, the averaged Green's functions and the propagator  $S(r, r')$  are given by Eqs. (A3) and (A4), and

$$P(r, r') = \frac{1}{\hbar^3 m^* D \tau^2 W L} \begin{cases} x(L - x') & x < x' \\ x'(L - x) & x > x' \end{cases}. \quad (\text{A9})$$

$F(r_1, r_2, r_3, r_4)$  is the short-ranged Hikami box [50] and in Fourier space is given by [29]

$$\begin{aligned} F(q_1, q_2, q_3, q_4) &= -m^* (\tau/\hbar)^5 v_F^5 (2\pi)^2 \delta(q_1 + q_2 + q_3 + q_4) \\ &\times [2(q_1 q_3 + q_2 q_4) + (q_1 + q_3)(q_2 + q_4)]. \end{aligned} \quad (\text{A10})$$

Performing all the integrals then gives the result

$$\begin{aligned} \langle |\nu(r, r', 1)|^2 \rangle &= 2 \left( \frac{m^*}{2\pi\hbar^2} \right)^2 \frac{1}{k_F l} \frac{1}{W L} \frac{x(L - x')}{L^2} p(x, x') \\ &= \frac{\nu_0^2}{g} \frac{x(L - x')}{L^4} p(x, x') \end{aligned} \quad (\text{A11})$$

with the abbreviation  $p(x, x') = (L - x)^2 + (L - x')^2 + \frac{1}{3}(x - x')^2 - \frac{2}{3}x'(L - x)$ . In the last step we used the Drude conductance  $g = k_F W l / 2L$ . The results for  $\langle |\nu(r, r', 2)|^2 \rangle$  and  $\langle \nu(r, r', 1) \nu(r', r, 2) \rangle$  are obtained using the same procedure.

## APPENDIX B: FINITE TEMPERATURE LINEAR RESPONSE RESULTS

For the configuration of figure 1, Eq. (27) gives the average current at the tip at fixed temperature and for given potentials  $\mu_\alpha$  at the massive contacts and  $\mu_{tip}$  at the tip. In this section we are interested in the case of finite temperature  $T$  and small applied bias such that  $kT \gg \Delta\mu$ . In this limit we can approximate the Fermi functions  $f_\alpha(E)$  in the reservoirs of the massive contact  $\alpha$  of the sample with the help of the Fermi function in the reservoir of the tip,

$$f_\alpha(E) \approx f_{tip}(E) - \frac{\partial f_{tip}}{\partial E} (\mu_\alpha - \mu_{tip}). \quad (\text{B1})$$

Using this expansion in (27) we get

$$\langle I_{tip} \rangle = \frac{e}{h} \sum_\alpha \int dE T_{ts}(x) \left( -\frac{\partial f}{\partial E} \right) \frac{\nu(x, \alpha)}{\nu(x)} (\mu_\alpha - \mu_{tip}) \quad (\text{B2})$$

with the Fermi function  $f(E)$  describing the distribution of electrons in the reservoir of the tip held at a potential  $\mu_{tip}$ . If we want to use the STM as a voltage probe we can easily solve the equation  $\langle I_{tip} \rangle = 0$  for  $\mu_{tip}$  and find

$$\mu_{tip} = \frac{\sum_\alpha \int dE T_{ts}(x) \left( -\frac{\partial f}{\partial E} \right) \frac{\nu(x, \alpha)}{\nu(x)} \mu_\alpha}{\int dE T_{ts}(x) \left( -\frac{\partial f}{\partial E} \right)}. \quad (\text{B3})$$

If one can take the fraction  $\nu(x, \alpha)/\nu(x)$  to be (nearly) independent of energy in an interval of size  $kT$  around the Fermi energy [49], equation (B3) reduces to the result valid at zero temperature, Eq. (30).

To find the finite temperature linear-response current fluctuation spectrum at the tip we have to insert the expansion (B1) into Eq. (32). This gives

$$\begin{aligned} \langle (\Delta I_{tip})^2 \rangle &= 4 \int dE G(x) \left( -\frac{\partial f}{\partial E} \right) \\ &\times \left\{ kT + f(E) \sum_\alpha \frac{\nu(x, \alpha)}{\nu(x)} (\mu_\alpha - \mu_{tip}) \right\}, \end{aligned} \quad (\text{B4})$$

where  $\mu_{tip}$  is adjusted according to Eq. (B3) such that the average current at the tip vanishes. The current fluctuations are the addition of pure thermal, Johnson-Nyquist noise,  $\langle (\Delta I_{tip})^2 \rangle_{therm} = 4G_{eff}(x)kT$  with the effective conductance  $G_{eff}(x) = \int dE G(x) (-\partial f / \partial E)$  and an excess noise proportional to the applied bias. Using an infinite impedance external circuit to measure the voltage at the tip, Eq. (24), gives the voltage fluctuation spectrum

$$\begin{aligned} \langle (\Delta V_{tip})^2 \rangle &= 4R_{eff}(x)kT \\ &+ 4R_{eff}(x)^2 \int dE G(x) \left( -\frac{\partial f}{\partial E} \right) f(E) \\ &\times \sum_\alpha \frac{\nu(x, \alpha)}{\nu(x)} (\mu_\alpha - \mu_{tip}) \end{aligned} \quad (\text{B5})$$

with the effective resistance  $R_{eff}(x) = [G_{eff}(x)]^{-1}$ .

- 
- [1] H.-L. Engquist and P. W. Anderson, Phys. Rev. B **24**, 1151 (1981).
  - [2] R. Landauer, Phil. Mag. **21**, 863 (1970); IBM J. Res. Develop. **1**, 223 (1957).
  - [3] M. Büttiker, Phys. Rev. Lett. **57**, 1761 (1986); IBM J. Res. Developm. **32**, 317 (1988).
  - [4] M. Büttiker, Phys. Rev. B **40**, 3409 (1989).
  - [5] T. Gramespacher and M. Büttiker, Phys. Rev. B **56**, 13026 (1997).
  - [6] Using Fermi Golden Rule arguments weak coupling contacts sensitive to currents (but not amplitudes) have been treated by Y. Imry, in *Directions in Condensed Matter Physics*, edited by G. Grinstein and G. Mazenko, (World Scientific Singapore, 1986). p. 101.
  - [7] G. Binnig and H. Rohrer, Helv. Phys. Acta **55**, 726 (1982); G. Binnig *et al.*, Phys. Rev. Lett. **49**, 57 (1982).
  - [8] *Scanning Tunneling Microscopy I,II,III*, Springer Series in Surface Sciences 20, 28, 29, Ed. by R. Wiesendanger and H.-J. Güntherodt (Springer, Heidelberg, 1992).
  - [9] Ph. Avouris, I.-W. Lyo, and Y. Hasegawa, IBM J. Res. Dev. **39**, 603 (1995), and other articles in the same issue.
  - [10] M. F. Crommie, C. P. Lutz, and D. M. Eigler, Science **262**, 218 (1993).
  - [11] L. C. Venema, J. W. G. Wildöer, J. W. Janssen, S. J. Tans, H. L. J. Temminck Tuinstra, L. P. Kouwenhoven, and C. Dekker, cond-mat/9811317.
  - [12] J. Tersoff and D. R. Hamann, Phys. Rev. B **31**, 805 (1985).
  - [13] J. Bardeen, Phys. Rev. Lett. **6**, 57 (1961).
  - [14] C. Bracher, M. Riza, and M. Kleber, Phys. Rev. B **56**, 7704 (1997).
  - [15] H. Pothier, S. Guéron, N. O. Birge, D. Esteve, and M. H. Devoret, Phys. Rev. Lett. **79**, 3490 (1997).
  - [16] M. Büttiker, J. Phys. Condens. Matter **5**, 9361 (1993).
  - [17] M. Büttiker and T. Christen, in: *Quantum Transport in Semiconductor Submicron Structures*, Ed. by B. Kramer, NATO ASI Series, Vol. **326** (Kluwer, Dordrecht, 1996), p. 263.
  - [18] T. Christen and M. Büttiker, Europhys. Lett. **35**, 523 (1996).
  - [19] Z. S. Ma, J. Wang, and H. Guo, Phys. Rev. B **57**, 9108 (1998).
  - [20] M. Büttiker, Phys. Rev. B **46**, 12485 (1992).
  - [21] M. J. M. de Jong and C. W. J. Beenakker, in: *Mesoscopic Electron Transport*, Ed. by L. L. Sohn, L. P. Kouwenhoven, and G. Schön, NATO ASI Series E, Vol. **345** (Kluwer, Dordrecht, 1997), p. 225.
  - [22] L. Saminadayar, D. C. Glatthli, Y. Jin, and B. Etienne, Phys. Rev. Lett. **79**, 2526 (1997).
  - [23] R. de-Picciotto, M. Heiblum, V. Umansky, G. Bunin, and D. Mahalu, Nature (London) **389**, 162 (1997).
  - [24] H. E. van den Brom and J. M. van Ruitenbeek, cond-mat/9810276.
  - [25] H. Birk, M. J. M. de Jong, and C. Schönenberger, Phys. Rev. Lett. **75**, 1610 (1995).
  - [26] M. Büttiker, Phys. Rev. Lett. **65**, 2901 (1990).
  - [27] M. Büttiker, Phys. Rev. Lett. **68**, 843 (1992).
  - [28] Th. Martin and R. Landauer, Phys. Rev. B **45**, 1742 (1992).
  - [29] Ya. M. Blanter and M. Büttiker, Phys. Rev. B **56**, 2127 (1997).
  - [30] E. V. Sukhorukov and D. Loss, Phys. Rev. Lett. **80**, 4959 (1998); cond-mat/9809239.
  - [31] S. A. van Langen and M. Büttiker, Phys. Rev. B **56**, R1680 (1997).
  - [32] M. P. Anantram and S. Datta, Phys. Rev. B **53**, 16390 (1996); S. Datta and P. F. Bagwell, and M. P. Anantram, Phys. Low-Dim. Struct. **3**, 1 (1996).
  - [33] M. Henny, S. Oberholzer, C. Strunk, and C. Schönenberger, (unpublished); M. Henny, Thesis (University of Basel, 1998).
  - [34] W. D. Oliver, J. Kim, R. C. Liu, and Y. Yamamoto, (unpublished).
  - [35] M. Büttiker, Physica B **175**, 199 (1991).
  - [36] R. C. Liu, B. Odom, Y. Yamamoto, and S. Tarucha, Nature **391**, 263 (1998).
  - [37] T. Gramespacher and M. Büttiker, Phys. Rev. Lett. **81**, 2763 (1998).
  - [38] S. Iida, H. A. Weidenmüller, and J. Zuk, Phys. Rev. Lett. **64**, 583 (1990); Ann. Phys. (N.Y.) **200**, 219 (1990).
  - [39] Note that the total charge consists of the injected charge and the screening charge due to the long range Coulomb interaction. See Ref. [16,17]. Here the charge generated by an external potential variation, keeping the internal potential fixed, is of interest.
  - [40] S. Datta, *Electronic Transport in Mesoscopic Conductors* (Cambridge University Press, Cambridge, England, 1995).
  - [41] P. Muralt and D. W. Pohl, Appl. Phys. Lett. **48**, 514 (1986).
  - [42] J. R. Kirtley, S. Washburn, and M. J. Brady, Phys. Rev. Lett. **60**, 1546 (1988).
  - [43] B. G. Briner, R. M. Feenstra, T. P. Chin, and J. M. Woodall, Phys. Rev. B **54**, R5283 (1996).
  - [44] G. Ramaswamy and A. K. Raychaudhuri, cond-mat/9812167.
  - [45] V. Gasparian, T. Christen, and M. Büttiker, Phys. Rev. A **54**, 4022 (1996).
  - [46] B. L. Altshuler and A. G. Aronov, in: *Electron-electron Interactions in Disordered Systems*, Ed. by A. L. Efros and M. Pollak (North-Holland, Amsterdam, 1985), p.1.
  - [47] K. E. Nagaev, Phys. Lett. A **169**, 103 (1992).
  - [48] C. W. J. Beenakker and M. Büttiker, Phys. Rev. B **46**, 1889 (1992).
  - [49] This is for instance the case if the energy intervall  $kT$  is smaller than the Thouless energy.
  - [50] S. Hikami, Phys. Rev. B **24**, 2671 (1981).